

Retinal Anatomy and Electrode Array Position in Retinitis Pigmentosa Patients After Argus II Implantation: An International Study



NINEL Z. GREGORI, NATALIA F. CALLAWAY, CATHERINE HOEPPNER, ALEX YUAN, ALEKSANDRA RACHITSKAYA, WILLIAM FEUER, HOSSEIN AMERI, J. FERNANDO AREVALO, ALBERT J. AUGUSTIN, DAVID G. BIRCH, GISLIN DAGNELIE, SALVATORE GRISANTI, JANET L. DAVIS, PAUL HAHN, JAMES T. HANDA, ALLEN C. HO, SUBER S. HUANG, MARK S. HUMAYUN, RAYMOND IEZZI JR, K. THIRAN JAYASUNDERA, GREGG T. KOKAME, BYRON L. LAM, JENNIFER I. LIM, NARESH MANDAVA, SANDRA R. MONTEZUMA, LISA OLMOS DE KOO, PETER SZURMAN, LEJLA VAJZOVIC, PETER WIEDEMANN, JAMES WEILAND, JIONG YAN, AND DAVID N. ZACKS

• **PURPOSE:** To assess the retinal anatomy and array position in Argus II retinal prosthesis recipients.

• **DESIGN:** Prospective, noncomparative cohort study.

• **METHODS:** **SETTING:** International multicenter study. **PATIENTS:** Argus II recipients enrolled in the Post-Market Surveillance Studies. **PROCEDURES:** Spectral-domain optical coherence tomography images collected for the Surveillance Studies (NCT01860092 and NCT01490827) were reviewed. Baseline and postoperative macular thickness, electrode-retina distance (gap), optic disc–array overlap, and preretinal membrane presence were recorded at 1, 3, 6, and 12 months. **MAIN**

OUTCOME MEASURES: Axial retinal thickness and axial gap along the array's long axis (a line between the tack and handle); maximal retinal thickness and maximal gap along a B-scan near the tack, midline, and handle.

• **RESULTS:** Thirty-three patients from 16 surgical sites in the United States and Germany were included. Mean axial retinal thickness increased from month 1 through month 12 at each location, but reached statistical significance only at the array midline ($P = .007$). The rate of maximal thickness increase was highest near the array midline (slope = 6.02, $P = .004$), compared to the tack (slope = 3.60, $P < .001$) or the handle (slope = 1.93, $P = .368$). The mean axial and maximal gaps decreased over the study period, and the mean maximal gap size decrease was significant at midline ($P = .032$). Optic disc–array overlap was seen in the minority of patients. Preretinal membranes were common before and after implantation.

• **CONCLUSIONS:** Progressive macular thickening under the array was common and corresponded to decreased electrode-retina gap over time. By month 12, the array was completely apposed to the macula in approximately half of the eyes. (Am J Ophthalmol 2018;193:87–99. © 2018 Published by Elsevier Inc.)

AJO.com

Supplemental Material available at AJO.com.

Accepted for publication Jun 13, 2018.

From the Bascom Palmer Eye Institute, University of Miami Miller School of Medicine, Miami, Florida, USA (N.Z.G., N.F.C., C.H., W.F., J.L.D., S.S.H., B.L.L.); Cole Eye Institute, Cleveland Clinic, Cleveland, Ohio, USA (A.Y., A.R.); USC Roski Eye Institute, University of Southern California, Los Angeles, California, USA (H.A., M.S.H., L.O.K.); The Wilmer Eye Institute, Johns Hopkins University School of Medicine, Baltimore, Maryland, USA (J.F.A., J.T.H.); Städtisches Klinikum, Augenklinik, Karlsruhe, Germany (A.J.A.); Retina Foundation of the Southwest, Dallas, Texas, USA (D.G.B.); Lions Vision Research and Rehabilitation Center, The Wilmer Eye Institute, Johns Hopkins University School of Medicine, Baltimore, Maryland, USA (G.D.); University Eye Clinic Luebeck at the University Hospital Schleswig-Holstein, Lübeck, Germany (S.G.); Duke University Eye Center, Durham, North Carolina, USA (P.H., L.V.); Wills Eye Hospital, Thomas Jefferson University, Philadelphia, Pennsylvania, USA (A.C.H.); Retina Center of Ohio, Cleveland, Ohio, USA (S.S.H.); Mayo Clinic, Rochester, Minnesota, USA (R.I.); Kellogg Eye Center, University of Michigan, Ann Arbor, Michigan, USA (K.T.J., J.W., D.N.Z.); Retina Consultants of Hawaii, Aiea, Hawaii, USA (G.T.K.); University of Illinois at Chicago, Chicago, Illinois, USA (J.I.L.); University of Colorado, Aurora, Colorado, USA (N.M.); University of Minnesota, Minneapolis, Minnesota, USA (S.R.M.); Eye Clinic Sulzbach, Knappschaft Hospital Saar, Sulzbach, Germany (P.S.); Klinik und Poliklinik für Augenheilkunde, Universitätsklinikum Leipzig, Leipzig, Germany (P.W.); Emory Eye Center, Emory University, Atlanta, Georgia, USA (J.Y.); and USC Ginsburg Institute for Biomedical Therapeutics, Los Angeles, California, USA (M.S.H.).

Lisa Olmos de Koo is currently at the University of Washington, Seattle, Washington, USA.

Paul Hahn is currently at New Jersey Retina, Teaneck, New Jersey, USA.

Inquiries to Ninel Z. Gregori, Bascom Palmer Eye Institute, 900 NW 17th St, Miami, FL 33136; e-mail: ngregori@med.miami.edu

THE ARGUS II RETINAL PROSTHESIS SYSTEM (SECOND Sight Medical Products, Inc., Sylmar, California, USA) is the first U.S. Food and Drug Administration–approved epiretinal implant that electrically stimulates the surviving inner retinal cells to induce visual perception in patients with severe retinitis pigmentosa (RP) and bare light perception or no light perception in both eyes.¹ RP causes a gradual destruction of photoreceptor cells; however, some bipolar, amacrine, and ganglion cells and their exons survive in these patients.^{1–4} The Argus II prosthesis has been shown to provide the recipients with some functional vision, useful in orientation and mobility tasks, and improve quality of life.^{1,5,6}

The Argus II retinal prosthesis consists of external components the patient wears, namely a pair of glasses with a

camera on the bridge of the nose and a video processing unit (VPU), which sends a digitized signal to the implant in the eye.⁴ The implant contains an electrode array with 60 200- μm platinum electrodes that deliver electrical stimulation to the surviving inner retina cells.⁴ The electrode array is affixed to the macula with a spring-loaded titanium tack. According to the surgeon's manual, the array should be centered over the fovea with electrodes oriented approximately 45 degrees diagonal to the horizontal meridian, aiming for either no overlap of the optic disc or overlap by the non-electrode portion of the array only.⁷ On the distal end of the array, opposite to the tack, is a handle, which consists of a circular tubing used for surgical manipulation of the array. Each electrode has an associated stimulation threshold, which quantifies the current required for the individual to perceive a phosphene.⁴

Previously published studies have focused on the implant's safety and efficacy. The landmark trial (Argus II Retinal Stimulation System Feasibility Protocol, NCT00407602) followed 30 patients throughout the United States, Europe, and Mexico, and reported an acceptable adverse events profile and improved ability to localize large objects and movement presented on a computer screen and to perform daily functions in a majority of patients up to 5 years after implantation.¹ Other studies have focused on factors that affect the perceptual thresholds. A significant correlation has been shown between stimulation threshold for perceiving phosphenes and the electrode-retina distance.⁴

There is, however, a paucity of data regarding changes in retinal anatomy after implantation, position of the electrode array relative to the retinal surface, and stability of the array position over time. A recent study of 18 eyes reported slight rotation of the array over time and variable electrode-retina distance with a surgical procedure adapted in France using scleral flaps and temporalis fascia autograft. Full apposition of the array was seen in a minority of patients.⁸ Position of the electrode array is dependent on the patient's anatomy, surgeon's technique, and relative difficulty in controlling the distance of the array from the retinal surface, especially in cases of high myopia or staphyloma.^{8,9}

The goal of this collaborative effort was to evaluate the spectral-domain optical coherence tomography (SD-OCT) images of the Argus II recipients enrolled in Post-Market Approval studies in the United States and international sites in order to assess the retinal anatomy and the array position in these patients. Based on clinical observations, we tested the hypothesis that with time the retina thickens in many patients, and the array-retina distance decreases, improving apposition of the array. This multicenter data analysis represents the largest longitudinal macular anatomy study in Argus II patients, and the procured information would aid in surgical planning, follow-up, and the development of future implant models with the overarching goal of improving artificial vision for

patients with severe vision loss owing to outer retinal degeneration.

METHODS

THE CURRENT STUDY IS A COLLABORATIVE EFFORT OF THE United States and international surgical sites participating in 2 of 3 Post-Market Surveillance Studies of the Argus II retinal prosthesis, which are prospective, interventional, open-label protocols (ClinicalTrials.gov identifiers NCT01860092 and NCT01490827). The aim of the current analysis was to review the SD-OCT images collected as part of Post-Market Surveillance Studies in order to evaluate the macular anatomy and electrode array position in these patients. All investigators of the 3 Post-Market Approval studies were invited, and only those centers who agreed to participate in this collaborative analysis were included (United States and German sites). Only data from patients who consented to participate in the Post-Market Surveillance Study in these centers were included. All subjects included in the current study had signed a consent form to be enrolled in the Post-Market Surveillance Study at their institution. Second Sight Medical Products, Inc provided access to de-identified images collected prospectively from baseline to month 12 after implantation as part of the Post-Market Study, which had been approved as a prospective study by an institutional review board or ethics committee at each institution and was compliant with the Health Insurance Portability and Accountability Act (HIPAA) or equivalent. All research was conducted in accordance with human subjects research standards and tenets of the Declaration of Helsinki.

Images were accessed via Second Sight's HIPAA-compliant, secure, encrypted account used in the Post-Market Surveillance Studies. The same SD-OCT (Spectralis OCT; Heidelberg Engineering, Inc, Heidelberg, Germany, or Cirrus OCT; Carl Zeiss Meditec Inc, Dublin, California, USA) was used to collect images at baseline and post-operatively for each individual patient. Retinal thickness and electrode-retina distance (the electrode-retina gap) were measured using the caliper tool on the respective SD-OCT system software. Measurement protocol was designed and de-identified OCT images were reviewed at the Bascom Palmer Eye Institute and Cole Eye Institute. The following parameters were investigated during 12 months after Argus II implantation: macular thickness changes; location (under or adjacent to the array) of macular thickening, if present; evolution of the retina-electrode distance through 1 year after implantation; correlation of the retina-electrode distance with the axial length; proximity of the array to the optic disc and the frequency and degree of optic nerve overlap; prevalence and characteristics of preretinal membranes before and after implantation.

Descriptive data were reviewed to study whether the retina was thickest under the array or outside of the array; how many eyes had retinal edema at baseline and how many developed retinal thickening after implantation of the Argus II; how often the preretinal membranes were present at baseline and how frequently they developed after implantation; whether the membranes caused tractional detachment or array misalignment; and whether the presence of the optic nerve overlap caused any optic nerve swelling.

A standardized approach to image evaluation and measurements was developed and strictly followed, as described below.

- **PREOPERATIVE MAXIMAL MACULAR THICKNESS:** Retinal thickness was measured as the distance from the inner retinal surface to the top of the hyperreflective layer under the retina, which anatomically represents the retinal pigment epithelium. Baseline maximal macular thickness was measured as the largest retinal thickness along a B-scan, in 3 locations: superior macula, foveal scan, and inferior macula. These locations approximated the location of the tack, the array midline, and the handle as closely as possible. Baseline maximal thicknesses at the superior macula, through the fovea, and at the inferior macula were compared to the maximal retinal thicknesses at the tack, midline, and handle, respectively at 1, 3, 6, and 12 months post-implantation.

- **POSTOPERATIVE AXIAL AND MAXIMAL MACULAR THICKNESS MEASUREMENTS:** Postoperative SD-OCTs at 1, 3, 6, and 12 months were analyzed. Retinal thickness was measured the same as preoperatively. The *axial* retinal thickness was measured on the best-quality OCT B-scan taken near the tack, the midline, and the handle at a point where the B-scan intersected the long axis of the array (a line running from the tack to the handle, as shown in Figure 1). In addition, the *maximal* retinal thickness was measured along these same B-scans in each of these 3 locations. It was documented whether the maximal measurement was located under the array and/or adjacent to the array. For all follow-up visits, a B-scan at a similar location with respect to the array anatomy was measured. If no scan of acceptable quality or correct location was available at a particular follow-up visit, no measurement was recorded to keep measurements consistent between visits.

- **MACULAR THICKENING:** Macular thickening was assessed as either present or absent at each follow-up visit by judging the appearance of retinal layers compared to baseline and earlier postoperative visits, and the location of thickening (quantified by the maximal macular thickness measurements) was documented as under the array and/or adjacent to the array. If the quality of the scan resolution under the array was sufficient, an attempt was made to distinguish whether intraretinal fluid cysts were present.

For all follow-up visits, a B-scan at a similar location was chosen at months 1, 3, 6, and 12.

- **AXIAL AND MAXIMAL ELECTRODE-RETINA GAP MEASUREMENTS:** The electrode-retina gap was defined as the distance between the inner retinal surface and the lower hyperreflective surface of the array marked by the shadows under the electrodes. The *axial* gap was measured on the same best-quality B-scans used for axial retinal thickness measurements near the tack, the midline, and the handle at a point where the B-scan intersected the long axis of the array (a line running from the tack to the handle, Figure 1). In addition, the *maximal* gap under the electrodes was measured on each of these B-scans at months 1, 3, 6, and 12.

- **OPTIC DISC OVERLAP:** The optic disc-to-array relationship was examined on the en face OCT images at each follow-up visit. Any presence or absence of optic nerve overlap was noted.

Among those with optic nerve overlap, the images were also assessed to determine if the disc was overlapped by the electrode-free polymer rim of the array (bumper) solely or also by the electrodes. The images were evaluated for evidence of optic nerve swelling by inspecting the appearance of the nerve rim on the en face images.

- **PRERETINAL MEMBRANE EVALUATION:** All available B-scans through the array at each visit were evaluated to detect any preretinal membranes. When a preretinal membrane was identified, it was classified as focal vs diffuse. Diffuse was defined as a membrane present on 5 or more contiguous B-scans. The membrane was also characterized as completely adherent vs focally adherent—that is, separated from the inner retinal surface (off the retina), if any separation was seen on any B-scan. Finally, the location of the preretinal membrane was described by quadrant (temporal, inferior, etc), hemifield if 2 contiguous quadrants, or diffuse if present in more than 2 macular quadrants, as much as possible, depending on the quality of OCT images.

- **STATISTICAL ANALYSIS:** Statistical analysis was performed using SPSS Version 24.0 (IBM Corp, Armonk, New York, USA). A *P* value of .05 or less was considered statistically significant. The Generalized Estimating Equations models employing a first-order autoregressive correlation structure were used to assess changes in thickness and gap size over time.

RESULTS

- **BASELINE PARTICIPANT DATA:** SD-OCT images of 33 patients from 16 surgical sites located in the United States

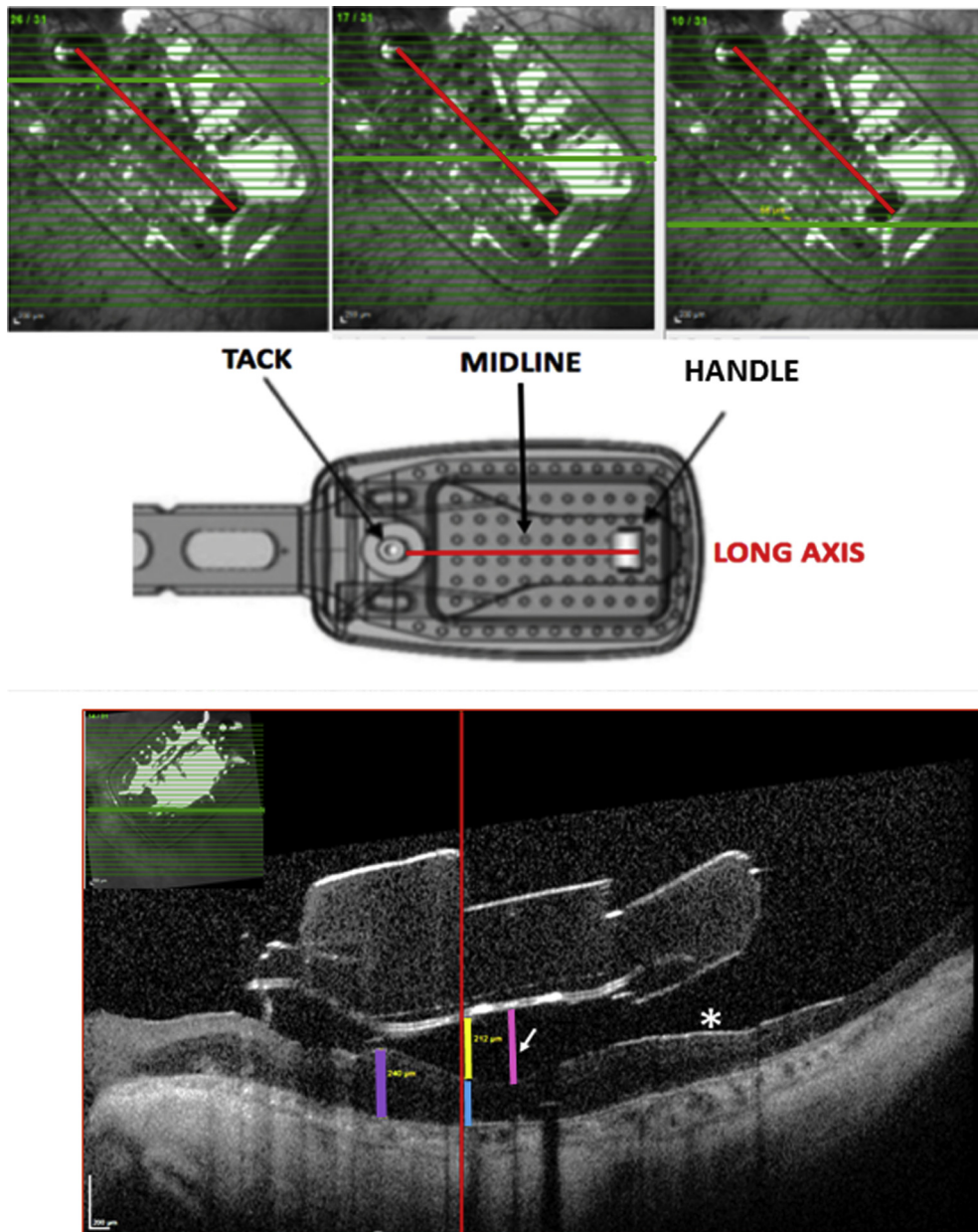


FIGURE 1. Measurement of Argus II optical coherence tomography (OCT) characteristics. (Top) En face OCT view of Argus II retinal prosthesis implant (Second Sight Medical Products, Inc, Sylmar, California, USA) with B-scan near the tack (Top left), midline (Top middle), and handle (Top right). (Middle) Illustration of the Argus II implant from the surgeon's manual labeled with the tack, midline, handle, and the array's long axis (red line) shown. The red line represents the long axis of the array used to measure axial thickness and gap. (Bottom) An OCT B-scan near the handle demonstrates how axial and maximal retinal thickness and electrode-retina gap were measured, and an example of an adherent preretinal hyperreflective membrane (asterisk *). The B-scan cuts through the array diagonally and thus the handle is not visible. The A-scan through the array's long axis is shown as a red vertical line. The blue line represents the axial macular thickness measurement. The yellow line represents the axial electrode-retina gap. The purple line shows the maximal retinal thickness along the B-scan. The pink line (indicated by the arrow) shows the maximal electrode-retina gap along the B-scan. Measurements were taken using the Heidelberg software program.

and Germany were reviewed from preoperative visit through month 12 after implantation, as available from Second Sight Medical Products, Inc. The baseline demographic information of participants is shown in [Table 1](#).

SD-OCT images were available for review as follows: 28 (85%) eyes had OCTs available at preoperative visit, 26 (79%) patients had OCTs from at least 2 postoperative visits, 17 (52%) patients had OCTs from at least 3 visits,

TABLE 1. Baseline Demographics of Participants

| Characteristic | Result |
|----------------------------------------------------------|----------------------------|
| Number of participants | 33 |
| Number of sites | 16 |
| Sex, n (%) | |
| Female | 10 (30%) |
| Male | 23 (70%) |
| Mean age \pm SD at time of implantation, years [Range] | 63 \pm 10 [46–88] |
| Laterality of implant, n (%) | |
| Right eye | 19 (58%) |
| Left eye | 14 (42%) |
| Mean axial length (mm) \pm SD [Range] | 23.2 \pm 1.0 [21.8–25.9] |
| SD = standard deviation. | |

and 9 (27%) patients had OCTs from all 4 postoperative visits.

• **AXIAL MACULAR THICKNESS ALONG THE ARRAY'S LONG AXIS:** In order to assess the macular thickness evolution under the array, the axial macular thicknesses along the long axis of the array, a line between the tack and the handle, were explored with spaghetti plots for each patient (data not shown), boxplots (Figure 2), and the mean axial thickness measurements near the handle, midline, and tack at different follow-up points (Table 2). Spaghetti plots and boxplots of the measurements at different follow-up points demonstrate a high variability between patients at each location (Figure 2). The median values in the boxplots are indicated by the horizontal line in the boxes encompassing data points in the 25th to the 75th quartiles. The median values remained fairly unchanged at the tack and the handle; however, they steadily increased at midline from month 1 through month 12. These findings were corroborated by the mean axial macular thicknesses (Table 2), which increase from month 1 through month 12 at each location, but reached statistical significance only at the array midline ($P = .007$).

• **MAXIMAL MACULAR THICKNESS BY LOCATION:** The maximal macular thicknesses near the tack, the midline, and the handle levels were measured along the same B-scan used to assess the axial macular thickness at these locations. Evolution of the maximal macular thickness after implantation was explored by spaghetti plots for each patient (data not shown), boxplots (Figure 3), and the mean maximal thicknesses at the handle, midline, and tack at different follow-up points (Table 2). The spaghetti plots and boxplots show large variability between patients. The median maximal macular thickness, represented by the horizontal line within boxes, increased from baseline through month 12 at each location, especially near the array midline (Figure 3). The mean maximal macular thicknesses increased from baseline at each location, and

reached statistical significance near the tack ($P < .001$) and midline ($P = .004$, Table 2). The rate of maximal thickness increase was highest near the array midline (slope = 6.02, $P = .004$), compared to the tack (slope = 3.60, $P < .001$) or the handle (slope = 1.93, $P = .368$).

• **MACULAR THICKENING:** Macular thickening was assessed as either present or absent at each follow-up visit by judging the appearance of retinal layers compared to baseline and earlier postoperative visits. Based on the appearance of the retinal layers and presence of cystic changes, 6 eyes out of 28 available baseline OCTs (21.4%) were classified as having macular edema prior to implantation. Five of 6 eyes had diffuse thickening (ie, present on more than 5 contiguous scans). After implantation, the macula appeared thickened in 11 of 21 (52%) eyes at month 1, 19 of 27 (70%) eyes at month 3, 13 of 19 (68%) eyes at month 6, and 16 of 18 (89%) eyes at month 12. To determine whether the retina thickened only under the array or also adjacent to the array, the location of the maximal macular thickness was recorded as under the array or outside, adjacent to the array in each OCT analyzed. Over the study period, the retina was thickest under the array in the majority of eyes (73%–96%); however, in up to a quarter of OCTs, namely 4%–27% of eyes (depending on the follow-up time point), the retina was thickest adjacent to the array, mostly in the nasal macula where the retina is naturally thicker than within the central macula at baseline, or where the array seemed to press on the adjacent retina, causing it to heap up immediately adjacent to the array edge, a “snowplow effect”. Resolution of many OCT scans was poor under the array, making it difficult to assess for the presence of cysts; thus these data are not reported. Almost none of the scans with adequate resolution showed cystic changes, but the retina appeared boggy. This was consistent throughout 12 months, with no specific trend noted at any location along the array.

• **ELECTRODE-RETINA GAP:** In order to assess the distance between the electrodes and the inner retina, the electrode-retina gap measurements were taken along the array's long axis near the tack, midline, and handle. In addition, the maximal gap measurements under the electrodes along the same B-scan near the tack, midline, and handle were recorded (Table 3). The boxplots demonstrate variability between eyes in the axial and maximal gap measurements (Figures 4 and 5). Along the long axis, the median axial gap was zero at all follow-up points near the tack and handle, while the median gap at midline was 165 μm at month 1 and steadily decreased to zero by month 12 (Figure 4). The median maximal electrode-retina gap was under 100 μm near the tack and the handle at month 1 and zero at other time points (Figure 5). The median maximal gap at midline was 214 μm at month 1 and steadily decreased to 40 μm by month 12 (Figure 5).

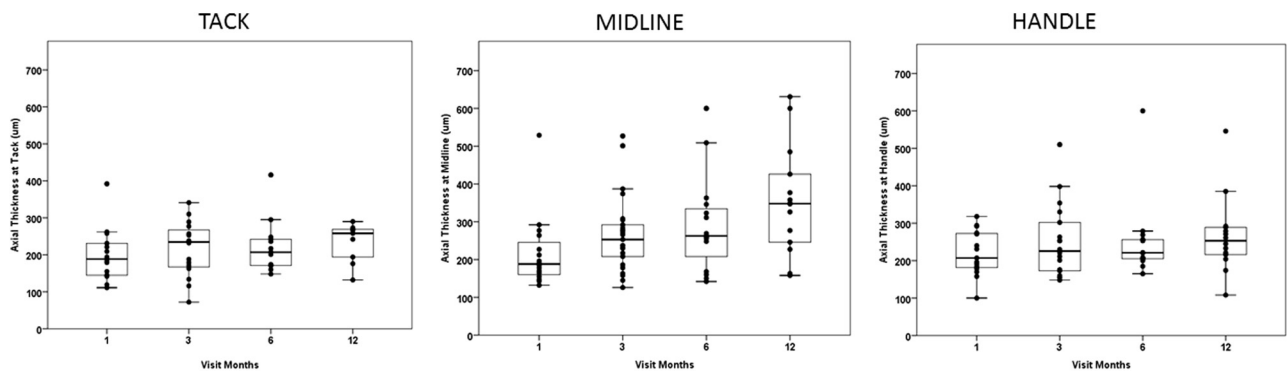


FIGURE 2. Axial macular thicknesses along array’s long axis by location through month 12 after Argus II implantation. Boxplots with Tukey’s quartiles are shown for the tack (Left), midline (Center), and handle (Right) with the measured retinal thickness in micrometers along the array’s long axis during postoperative months 1, 3, 6, and 12. The median value is indicated by the horizontal line in the box encompassing data points in the 25th to the 75th quartiles. The median values remained fairly unchanged at the tack and the handle, but steadily increased at midline from month 1 through month 12. The x-axis represents months after surgery; the y-axis represents thickness in micrometers (μm).

TABLE 2. Axial and Maximum Macular Thickness by Array Location Through Month 12 After Argus II Implantation

| Visit | Tack | | Midline | | Handle | |
|---------------------------|----------------------------------------------------------|---------------------------------------------------------|----------------------------------------------------------|---------------------------------------------------------|----------------------------------------------------------|---------------------------------------------------------|
| | Mean Axial Thickness Along Long Axis, μm (SD) | Mean Maximal Thickness Along B-Scan, μm (SD) | Mean Axial Thickness Along Long Axis, μm (SD) | Mean Maximal Thickness Along B-Scan, μm (SD) | Mean Axial Thickness Along Long Axis, μm (SD) | Mean Maximal Thickness Along B-Scan, μm (SD) |
| Baseline ^a [n] | | 230.9 (59.8) [20] | | 236.5 (51.5) [23] | | 233.8 (46.4) [19] |
| POM1 [n] | 200.1 (73) [14] | 227.5 (60.7) [16] | 216.4 (96.2) [16] | 269.3 (85.4) [16] | 220.3 (60.7) [15] | 266.1 (79.4) [16] |
| POM3 [n] | 216.1 (74) [16] | 272.8 (88.8) [16] | 265.5 (98.9) [25] | 290.4 (89.2) [25] | 249.6 (97.8) [18] | 280.4 (97.5) [19] |
| POM6 [n] | 222 (71.7) [13] | 254.4 (64.7) [13] | 289.3 (124.7) [16] | 337.5 (118) [16] | 248.7 (102.5) [15] | 302.3 (114.6) [15] |
| POM12 [n] | 233.3 (53.5) [9] | 279.9 (35.3) [9] | 355 (144) [14] | 389.4 (134.4) [14] | 266 (102.8) [14] | 317.2 (96.2) [14] |
| Slope ^b (SE) | 0.95 (1.68) | 3.60 (0.81) | 7.79 (2.91) | 6.02 (2.08) | 0.25 (1.63) | 1.93 (2.14) |
| P value | .573 | <.001* | .007* | .004* | .881 | .368 |

POM = postoperative month; SD = standard deviation; SE = standard error.

Statistically significant P values are indicated by an asterisk (*).

^aFor baseline maximal retinal thickness the maximal thickness along B-scan in the superior macula (ie, near tack), through the fovea (ie, near array midline), and in the inferior macula (ie, near handle) were measured.

^b($\mu\text{m}/\text{month}$) Generalized Estimating Equations model accounting for correlated measurements on the same subjects with visit months fitted as a linear covariate (excluding baseline) with identity link and correlation structure modeled as AR1.

The majority of eyes had complete touch of the electrodes and the retina (zero gap) at the tack and the handle (Table 4). The percentage of eyes with zero axial and maximal gap increased significantly across the follow-up visits at the midline but not at the tack or the handle, which corresponds to the significant macular thickening at array midline seen postoperatively. While the mean axial and maximal gaps decreased over the study period, the decrease in mean maximal gap size at midline was the only significant trend observed ($P = .032$, Table 3).

A negative correlation between the electrode-retina gap change and macular thickness change along long axis of the array was observed from month 1 to month 3 ($n = 11$, $r = -0.69$, $P = .019$), from month 1 to month 6 ($n = 10$,

$r = -0.79$, $P = .007$), and from month 1 to month 12 ($n = 9$, $r = -0.83$, $P = .006$).

• CORRELATION OF ELECTRODE-RETINA GAP WITH AXIAL LENGTH AND TACK APPEARANCE: Axial length ranged from 21.8 mm to 25.9 mm, with a median of 23.2 mm. Axial length was not correlated with large maximal gap. Axial lengths as small as 22.0 mm and as large as 25.91 mm were represented among the eyes with a maximal gap larger than 150 μm and larger than 200 μm at any location. Moreover, the 22.0 mm eye had larger gaps at the tack, midline, and handle than the 25.91 mm eye.

Out of 10 eyes with the maximal electrode-retina gap of 150 μm or more at the midline or the handle at month 1, 5

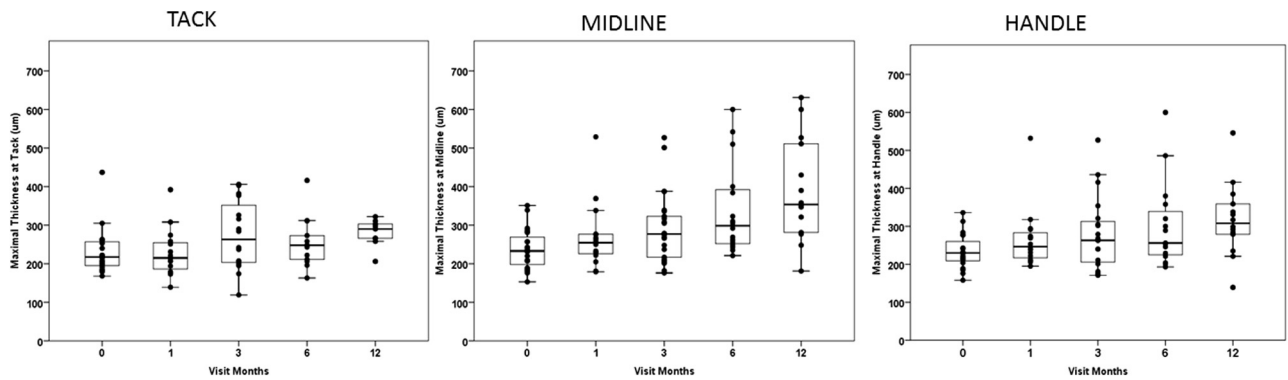


FIGURE 3. Maximal macular thicknesses along the b-scan by location through month 12 after Argus II implantation. Boxplots with Tukey’s quartiles are shown for the tack (Left), midline (Center), and handle (Right) with the maximum retinal thickness along the B-scan measured in micrometers at postoperative months 1, 3, 6, and 12. The median value is indicated by the horizontal line in the box encompassing data points in the 25th to the 75th quartiles. The x-axis represents months after surgery; the y-axis represents thickness in micrometers (μm).

TABLE 3. Mean Axial and Mean Maximal Electrode-Retina Gap by Array Location Through Month 12 After Argus II Implantation

| Visit | Tack | | Midline | | Handle | |
|----------------------|----------------------------------------------------|----------------------------------------------|----------------------------------------------------|----------------------------------------------|----------------------------------------------------|----------------------------------------------|
| | Mean Axial Gap Along Long Axis, μm (SD) | Mean Max Gap Along BScan, μm (SD) | Mean Axial Gap Along Long Axis, μm (SD) | Mean Max Gap Along BScan, μm (SD) | Mean Axial Gap Along Long Axis, μm (SD) | Mean Max Gap Along BScan, μm (SD) |
| POM1 [n] | 73.7 (131.8) [15] | 86.9 (107.8) [14] | 167 (156.8) [16] | 188.1 (163.6) [16] | 66.1 (79.9) [15] | 154.5 (152.1) [15] |
| POM3 [n] | 39.8 (85.8) [16] | 59.1 (110) [16] | 116.2 (140.9) [25] | 149.8 (148.6) [25] | 52.5 (84.9) [18] | 88.8 (115.3) [19] |
| POM6 [n] | 28.2 (51.5) [13] | 47.5 (79.2) [13] | 72.6 (107.1) [16] | 98.7 (114.8) [16] | 49.9 (84.7) [15] | 78.7 (110) [15] |
| POM12 [n] | 60.6 (119.4) [9] | 76.0 (124.8) [9] | 87.0 (150.7) [14] | 116.5 (146.7) [14] | 62.7 (80.6) [14] | 91.8 (99.5) [14] |
| Slope (SE) | -0.75 (0.87) | -0.22 (2.41) | -3.84 (2.41) | -4.84 (2.26) | -0.14 (2.12) | -2.92 (2.91) |
| P value ^a | .393 | .927 | .111 | .032* | .948 | .315 |

POM = postoperative month; SD = standard deviation; SE = standard error.

Statistically significant P values are indicated by an asterisk (*).

^a($\mu\text{m}/\text{month}$) Generalized Estimating Equations model accounting for correlated measurements on the same subjects with visit months fitted as a linear covariate (excluding baseline), with identity link and correlation structure modeled as AR1.

had zero axial gap at the tack (ie, no separation between the array and the retina at the tack). Interestingly, 3 of these 5 eyes had a large maximal gap of 85, 108, and 185 μm near the tack at month 1, indicating a degree of tilt of the array around the long axis. The 5 remaining eyes demonstrated tack gaps between 32 and 395 μm at month 1. The eye with a 395- μm gap at the tack had the largest axial gap and maximal gap at the midline (both 483 μm). Two eyes had a steep curvature of the macula but axial lengths of 24.2 and 23.7 mm and no obvious staphyloma on preoperative examination, with a large maximal electrode-retina gap of 433 and 483 μm at the midline, respectively (Figure 6, Middle right). Thus, it appears that in some eyes incomplete tacking was responsible for the large electrode-retina gap, and in other eyes the curvature of the array and the retina did not follow the same radius,

while in some eyes the array appeared tilted in such a way that 1 edge lifted off the retina.

- **OPTIC NERVE-ARRAY OVERLAP:** Optic disc overlap was observed in 8 of 19 (42%) OCTs at month 1, 8 of 26 (31%) at month 3, 3 of 18 (17%) at month 6, and 5 of 18 (28%) OCTs at month 12. In the majority of eyes the overlap was by the electrode-free polymer rim only. A single electrode was seen over the optic nerve in 2 eyes at month 1, 1 eye at month 3 (1 of the 2 eyes from month 1), and 1 eye at month 12 (a different eye, which was not imaged earlier). No evidence of optic nerve edema was visible in any of the images.

- **PRERETINAL HYPERREFLECTIVE MEMBRANES:** Completely adherent, very fine hyperreflective membranes

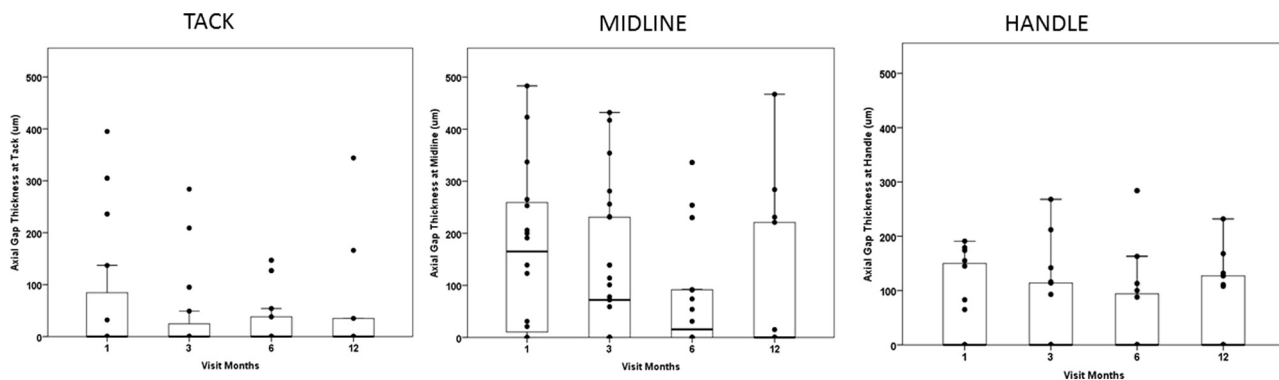


FIGURE 4. Axial electrode-retina gap along array's long axis by location through month 12 after Argus II implantation. Boxplots with Tukey's quartiles are shown for the tack (Left), midline (Center), and handle (Right) with the electrode-retina distance (gap) measured in micrometers during postoperative months 1, 3, 6, and 12. The median value is indicated by the horizontal line in the box encompassing data points in the 25th to the 75th quartiles. Median gap was zero near the tack and the handle at all points, and steadily decreased at midline from month 1 through month 12. The x-axis represents months after surgery, the y-axis represents thickness in microns.

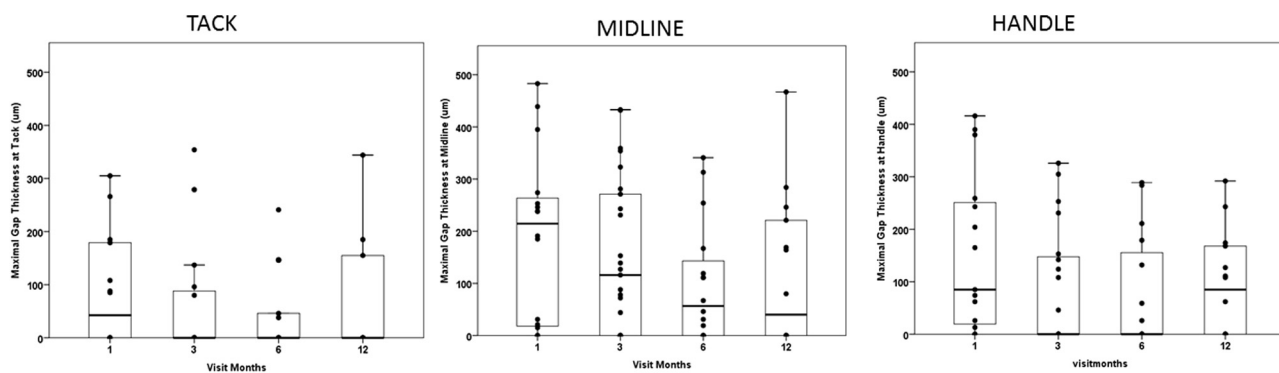


FIGURE 5. The maximal electrode-retina gap along the B-scan by location through month 12 after Argus II implantation. Boxplots with Tukey's quartiles are shown for the tack (Left), midline (Center), and handle (Right) with the electrode-retina distance (gap) measured in micrometers during postoperative months 1, 3, 6, and 12. The median value is indicated by the horizontal line in the box encompassing data points in the 25th to the 75th quartiles. The median maximal gap was under 100 microns near the tack and the handle at month 1 and zero at most other time points. The median maximal gap at midline was 214 microns at month 1 and steadily decreased to 40 microns by month 12. The x-axis represents months after surgery, the y-axis represents thickness in microns.

were seen in 25 of 28 (89%) eyes at baseline (Figure 6, Top left), 14 of 15 (93%) eyes at month 1, 19 of 21 (90%) eyes at month 3, 12 of 13 (92%) at month 6, and 13 of 14 (93%) eyes at month 12. These adherent membranes were diffusely present in 5 or more contiguous B-scans in 20 of 25 (80%) eyes at baseline, 13 of 14 (93%) eyes at month 1, 18 of 19 (95%) eyes at month 3, 11 of 12 (92%) eyes at month 6, and 11 of 12 (92%) eyes at month 12. These fine, completely adherent membranes were seen everywhere in the macula in 76%, 57%, 65%, 67%, and 58% at baseline and months 1, 3, 6, and 12, respectively.

Off-the-retina focally adherent membranes were seen in 10 of 28 (36%) eyes at baseline, 6 of 15 (40%) eyes at month 1, 9 of 21 (43%) eyes at month 3, 5 of 13 (38%) eyes at month 6, and 10 of 14 (71%) eyes at month 12

(Figure 6, Middle left). These membranes were diffusely present in 5 of 9 (56%) eyes at baseline, 4 of 6 (67%) eyes at month 1, 4 of 9 (44%) eyes at month 3, 4 of 5 (80%) eyes at month 6, and 8 of 9 (89%) eyes at month 12. The off-the-retina membranes were seen in 1 or 2 quadrants only in 67% eyes at baseline and all eyes at months 1 through 12 postoperatively.

Preoperatively only 4 eyes demonstrated a thick focally adherent off-the-retina preretinal membrane resembling a true epiretinal membrane or thick hyaloid (Figure 6, Top center), and these were no longer present after vitrectomy and implantation surgery. Postoperatively all completely adherent and most off-the-retina focally adherent membranes were very fine and were not seen to affect the position of the array (Figure 6, Middle left), with only 1 eye

TABLE 4. Number (Percentage) of Eyes With Complete Electrode-Retina Touch (Zero Electrode-Retina Gap)

| Visit | Tack | | Midline | | Handle | |
|-----------------------------|---------------------|----------------------|---------------------|----------------------|---------------------|----------------------|
| | Along Axis N (%) | Maximum Gap N (%) | Along Axis N (%) | Maximum Gap N (%) | Along Axis N (%) | Maximum Gap N (%) |
| POM1 | 10 (67%) | 7 (50%) | 4 (25%) | 3 (19%) | 8 (53%) | 3 (20%) |
| POM3 | 12 (75%) | 11 (69%) | 11 (44%) | 8 (32%) | 12 (67%) | 10 (53%) |
| POM6 | 9 (69%) | 8 (62%) | 8 (50%) | 5 (31%) | 10 (67%) | 8 (53%) |
| POM12 | 6 (67%) | 6 (67%) | 9 (64%) | 7 (50%) | 8 (57%) | 6 (43%) |
| <i>P</i> value ^a | .334 | .854 | .006* | .020* | .953 | .577 |

POM = postoperative month.

The number and frequency of eyes with no measureable gap on optical coherence tomography (OCT) imaging are reported at the three recorded array locations both in the long axis of the array and the maximal gap identified on the same B-scan. The midline, along the array of the axis, demonstrated a statistically significant increase in the frequency of zero electrode-retina gap over time after implantation of the array ($p=0.006$). The axial midline measurement approximates the foveal location.

Statistically significant *P* values are indicated by an asterisk (*).

^aA *P* value for trend over time Generalized Estimating Equations logistic link AR1 correlation matrix, linear fit.

showing an off-the-retina membrane elevating an edge of the array off the retina. No tractional membranes were seen. Two eyes with peculiar hyperreflective layer adherent to the posterior surface of the array separate from the retina were seen, which may represent either fibrosis or inflammatory material (Figure 6, Middle center). No membranes encapsulating the array were seen in any eyes.

DISCUSSION

PROGRESSIVE MACULAR THICKENING UNDER THE ARRAY was commonly seen and corresponded to decreased electrode-retina gap from month 1 to month 12 after implantation. By month 12, the array was well apposed to the macula, with no gap from the tack to the handle, in approximately half of the eyes. In the majority of eyes the retina was thickest under the array, but in some eyes at each follow-up period the retina was thickest adjacent to the array owing to a “snowplow” effect of the array’s edge pressing against the retina (Figure 6, Bottom left). Since a significant correlation has been shown between electrode thresholds for eliciting visual percepts and the electrode-retina distance,⁴ the current needed to create a phosphene would be expected to be lower the closer the implant is to the retina. Ahuja and associates studied 22 Argus II patients and showed that placing the array in close proximity to the retinal surface produced a high percentage of electrodes with lower thresholds.⁴ De Balthasar and associates studied 6 patients with an earlier version of the Argus implant and demonstrated direct correlation of stimulation thresholds with the distance from the retinal surface but not with electrode size, electrode impedance, or retinal thickness.¹⁰

It would have been informative to study a correlation between the electrode-retina gaps and the electrode thresholds in this study; however, the Post-Market Surveillance Studies do not require rechecking of electrode thresholds at any point. The patients were reprogrammed on an “as needed” basis as requested by individual sites, whenever a patient reported discomfort or declining visual function or did not respond well to the current settings. Thus, we were unable to collect and systematically analyze device functional data in relation to the changes in anatomy.

We also considered comparing thresholds between patients with and without complete apposition; however, that analysis would be inconclusive since thresholds in each individual depend on many factors: the apposition gap between the retina and the array, the health of the residual cells, possible membranes under the array, time given between stimulations (cell recovery time), patient fatigue during a testing session, and possibly age and number of years of blindness. Moreover, comparing visual function, as measured by 3 custom-designed primary endpoints used in the Surveillance Studies (square localization, direction of motion, and grating visual acuity),¹ would introduce a bias of blind rehabilitation training over time.

Based on the imaging results of the current study, it appears prudent to monitor the array position and macular anatomy in the retinal prosthesis recipients over time with OCT. Since the initial programming usually occurs at 2–4 weeks after implantation, if a significant change in the retina-electrode distance or a new membrane is detected, it may be helpful to reprogram the device, for example at 6–12 months, to adjust the currents based on the anatomy of the patient. Patient comfort and quality of phosphenes may improve after reprogramming, and should be a subject of a future study looking specifically at device function in relation to retinal anatomy and array positioning.

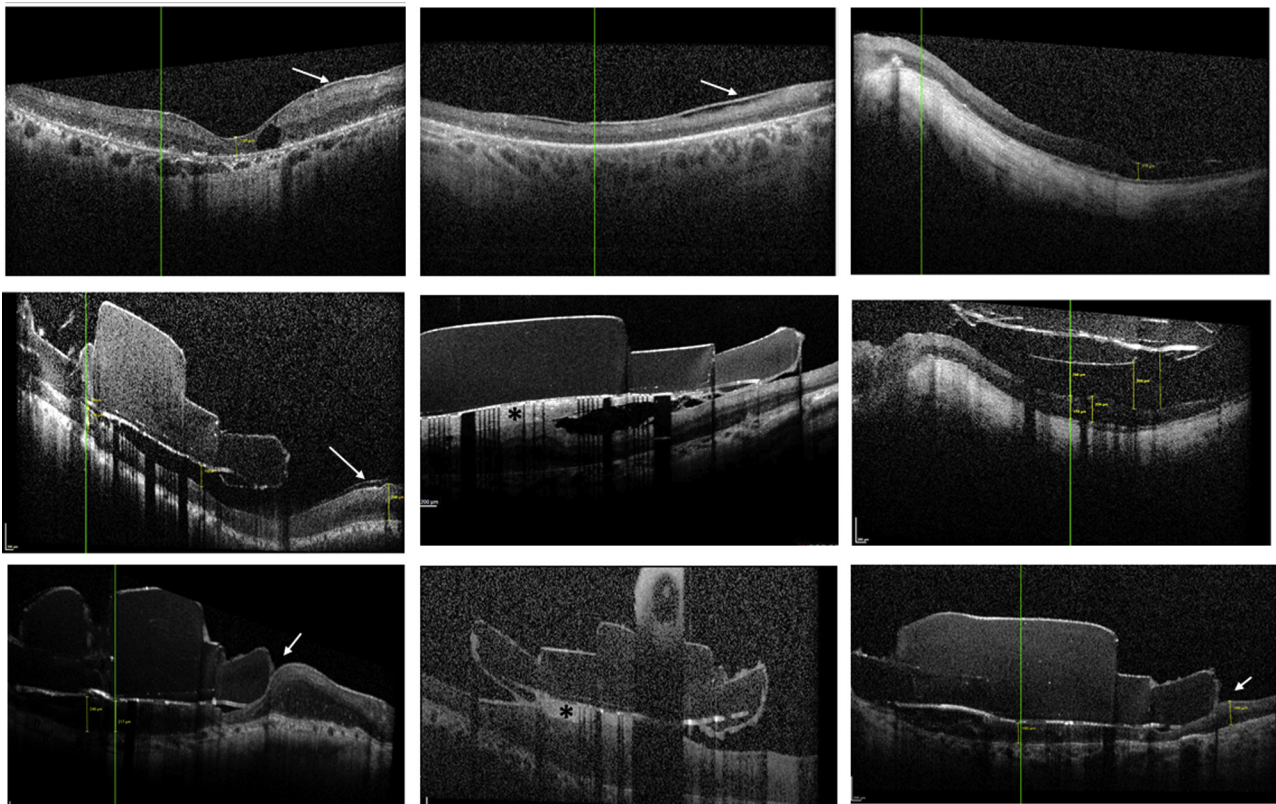


FIGURE 6. Representative optical coherence tomography (OCT) scans at baseline and after Argus II retinal prosthesis implantation. (Top left) Baseline OCT scan shows intraretinal cyst and completely adherent hyperreflective preretinal membrane (arrow). (Top center) Baseline OCT scan shows an example of a thick off-the-retina membrane (arrow) resembling either an epiretinal membrane or thick hyaloid. (Top right) Baseline OCT scan shows macular concavity in a patient with one of the largest electrode-retina gaps (359 microns maximal gap at midline at month 1). (Middle left) OCT scan shows low-lying off-the-retina membrane (arrow) commonly seen after Argus II implantation. (Middle center) OCT scan shows a peculiar hyperreflective layer (asterisk *) adherent to the posterior surface of the array separate from the retina, which may represent either fibrosis or inflammatory material. Thickened retina is seen below the hyperreflective layer. (Middle right) OCT scan at month 1 shows one of the largest maximal electrode-retina gaps (433 microns at midline) in the eye with a macular concavity shown in top right image. (Bottom left) OCT scan shows a “snowplow” effect of the array pressing against the retina (arrow) and causing adjacent thickening. (Bottom center) OCT example of boggy macular thickening under the array and hyperreflective layer (asterisk *) under the array. OCT quality is not sufficient to distinguish if cysts are present. (Bottom right) OCT example of the array completely apposed against the retina. No retinal thickening is seen in this scan. Mild “snowplow” effect is visible (arrow).

Optic disc–array overlap by the polymer rim was seen in up to 40% of eyes, depending on the time point, with a single electrode visible over the optic nerve in a total of 3 eyes only, and no optic nerve edema was detected. Thus, the surgical placement appears to follow the surgical manual adequately, without obvious optic nerve compromise.

Preretinal membranes were present in almost all OCT scans at baseline and all postoperative follow-up periods. A third or more of eyes also had membranes separated from the retina before and after surgery. The adherent and off-the-retina membranes were present with similar frequency and characteristics at all postoperative follow-up periods, and no tractional or encapsulating membranes were seen. Based on our surgical experience, RP patients

have a very adherent cortical vitreous, which fragments into wisps and may be difficult to remove completely; thus, the preretinal membranes may represent the adherent hyaloid and its postoperative remnants.

Two eyes with “subclinical staphyloma” evident as a steep macular concavity on preoperative OCT had large electrode-retina gaps, which did not prevent functionality of the device in these 2 patients. Both patients performed better with the device ON than OFF on Square Localization testing. Large electrode-retina gap under the array’s midline was seen in eyes with incomplete tacking, steep macular concavity, or tilting of the array with 1 edge lifting off the retina. The currently approved Argus II epiretinal prosthesis contains a semi-rigid polymer array, which has

some flexibility but may not follow the curvature of the posterior retina completely, resulting in variability of the electrode-retina distance.¹¹

At the time when the current study was planned and the collaborative group was formed, no large-scale published studies evaluated the macular anatomy and array position in the retinal prosthesis recipients. The idea for this collaborative project was born during an investigators meeting held at ARVO in 2016. The current study was designed to assess the macula and the array position as a variable of time with an overarching goal to understand whether the current design of the array allows close contact between the electrodes and the retina or whether a modification of the current array is necessary.

Our data demonstrated that the current array is able to appose the retina in about half of the patients; however, more flexible design may improve the electrode-retina proximity in patients with steep maculae. A recent report from 3 French implanting sites, using a modified surgical implantation technique involving construction of a scleral flap, showed complete apposition of the Argus II array to the retina in only 4 of 18 (22.22%) eyes, partial apposition in 9 of 18 (50%), and lack of apposition in 5 eyes (27.78%), 4 of which had a posterior staphyloma and 1 of which had a concave macula without an obvious staphyloma.⁸ The mean electrode-retina distances in that study were between 100 and 450 μm in patients with partial apposition, with the largest gap seen in the eye with incomplete insertion of the retinal tack.⁸ In the current study, a concave macula and poor insertion of the retinal tack were also associated with the largest electrode-retina gaps. We further explored a possibility that long axial lengths may make it difficult for the surgeon to handle the array over the retina; however, large electrode-retina gaps did not correlate with the long axial lengths, as long as 25.9 mm, in our cohort.

OCT has been shown to be an essential tool for screening potential retinal prosthesis candidates, mainly to identify a posterior staphyloma or significant epiretinal membrane, and more recently as an intraoperative tool to guide the surgeon during array tacking.^{9,11,12} We used SD-OCT to examine changes in the macular thickness after Argus II implantation. In our cohort, 21% of eyes demonstrated cystic macular edema prior to implantation. By 12 months, 89% of eyes had some degree of macular thickening compared to baseline retinal appearance and thickness, which may be owing to long-term mechanical or electric stimulation of the retina, and may be nonpathologic. Interestingly, electrical stimulation to the retina has been shown to lead to preservation of the retinal cells via generalized neurotrophic effect. For example, transcorneal electrical stimulation was found neuroprotective against light-induced retinal degeneration in rodents, with cell preservation seen in the inner and outer retinal layers, including increased survival of ganglion cells.^{13–15} Subretinal electrical stimulation by the artificial silicon retina microchip with 5000 microelectrodes has been

shown to improve visual field size, visual acuity, and subjective visual function distant to the implant in a pilot study with 6 patients followed for over 1 year.¹⁵ Electrical stimulation of the retina has been shown to lead to downregulation of proapoptotic factors and release of neurotrophic factors.^{14,16,17} Moreover, electrical stimulation can promote ganglion cell growth and regeneration in vitro and in vivo.¹⁸ Increase in the retinal thickness in response to electrical stimulation has been shown in an in vivo rabbit model with platinum/iridium disk electrodes.¹⁹ The authors demonstrated retinal swelling after 30 minutes of high-density electrical stimulation at 1.22 and 1.63 mC/cm^2 but not with lower charge densities of 0.92 and 1.02 mC/cm^2 .¹⁹ The Argus II stimulation limit is 0.35 mC/cm^2 , which is well within the safety limits of up to 1 mC/cm^2 shown to be safe with the Argus II implant.⁴ Thus, the nature of macular thickening observed in the retinal prosthesis recipients is not clear and should be studied further, possibly by clinicopathologic correlations as opportunities arise.

There are inherent limitations to our study. Baseline macular thickness was measured in the superior macula, through the fovea, and in the inferior macula, approximating the locations of the tack, the midline, and the handle. Direct correlation of the locations was not possible owing to inability to register fundus images and OCT images before and after implantation. Other limitations to note are relatively small sample size and the impact of potential loss to follow-up on the data, making it difficult to assess longitudinal outcomes over time. The reader should keep in mind that each point is a cross-sectional survey of the available measurements and not the data from all 33 patients.

Another limitation of the current study is inconsistent quality of the OCT images. Given poor fixation, significant nystagmus, and high reflectivity of the array, obtaining good-quality scans is not trivial in these patients. Owing to inconsistent quality of the images, it was not possible to adequately visualize the retinal layers and evaluate for possible cysts in many scans. The 6 mm \times 6 mm images obtained with commercially available SD-OCT systems may not produce a clear view of the underlying retina or capture the entire nasal-to-temporal view of the array. The swept-source OCT has been shown to produce superior images of the Argus II array and the underlying retina owing to higher image acquisition speed, deeper penetration into the retina, longer wavelength with better signal-to-noise ratio, and wide-field 12 mm \times 12 mm images.²⁰ Unfortunately, swept-source OCT devices are not widely available and were not used in the Surveillance Studies. Moreover, no standardized OCT protocol was required in the Surveillance Studies.

In conclusion, we demonstrate significant macular thickening under the array midline and corresponding significant decrease in the maximal retina-electrode gap over 12 months after Argus II implantation. The gap diminished with time in many eyes and became zero in approximately

half of the eyes at 1 year. While the current study was not able to evaluate the effects of the retina-electrode positioning on the electrode function, it described a dynamic nature of the anatomy in the retinal prosthesis recipients. Monitoring the array position and macular anatomy in

these patients provides the clinician valuable information regarding the array positioning, which may suggest an appropriate time for reprogramming of the electrode currents and increase our understanding of the biomechanics of the retinal implants.

FUNDING/SUPPORT: SUPPORTED BY VITREORETINAL SURGERY FOUNDATION (MINNEAPOLIS, MINNESOTA) AWARD (TO NATALIA Callaway and Ninel Z. Gregori), NIH Center (Bethesda, Maryland) Core Grant P30EY014801, Research to Prevent Blindness (New York City, New York) Unrestricted Grant, Department of Defense (Washington, DC) (DOD-Grant#W81XWH-09-1-0675). The sponsor or funding organizations had no role in the design or conduct of this research. Second Sight Medical Products, Inc, provided funding for the Post-Market Surveillance Study to individual institutions but did not directly sponsor or influence the current work. Financial Disclosures: Ninel Z. Gregori: Regeneron, Inc (consultant). Alex Yuan: Second Sight Medical Products, Inc (research grant), NIH/NEI K08 EY023608 (unrelated grant). Aleksandra Rachitskaya: Allergan, Carl Zeiss Meditec (consultant). William Feuer: National Eye Institute (grants: U10EY024247 and P30EY014801); Johnson and Johnson (grant); Glaucoma Associates of Texas, Retinal Care LLC, Tissue Tech (consultant). Hossein Ameri: Second Sight (USC grant for clinical trials), Spark Therapeutics (advisory board). J. Fernando Arevalo: Springer SBM LLC (royalties); EyEngineering Inc, Turing Pharmaceuticals LLC, Mallinckrodt (consultant); Dutch Ophthalmic Research Consultants International B.V., Allergan Inc, Bayer (consultant, lecture fees). Albert J. Augustin: Allergan, Alimera (consultant, speakers honoraria, study grants); Novartis, Bayer (study grants); Second Sight Medical Products, Inc (speakers honoraria, study grants). David G. Birch: Nightstar, Inc, AGTC, Nacuity Pharmaceuticals, Acucela, Inc (consultant); Nightstar, Inc, Ionis Pharmaceuticals, Inc, Allergan, AGTC, 4D Molecular Therapeutics, Inc, Second Sight Medical Products, Inc (clinical trial support). Gislin Dagnelie: Second Sight Medical Products (consulting, patents, clinical trial funding); QLT Inc [now Novelon] (consulting, licensing fees); eSight Corp (consulting, equity); grants NIH R01 EY028452, R42 EY025136, R44 EY024498, R44 EY027650, UG3 NS095557 and DoD W81XWH-17-1-0621. Salvatore Grisanti: Alcon, Allergan, Bayer, Humanoptics, Novartis, Pfizer, Roche, Transcend (advisory boards, presentation, studies); Refocus, Thrombogenics (studies). Janet L. Davis: Abbvie, Allergan (consultant). Paul Hahn: Second Sight Medical Products, Inc, Genentech, Inc (consultant). James T. Handa: Bayer Pharmaceuticals, Inc, NIH R01 EY027691, NIH 2R01 EB000526-07, BrightFocus Foundation, Macular Degeneration Foundation, Knights Templar Grant (unrelated grants). Allen C. Ho: Aerie Pharmaceuticals, AsclepiX Therapeutics, Beaver Visitec, BioTime, Kang Hong Biotech, Novo Nordisk, Notal Vision, Tyrogenex (consulting); AGTC, Alcon, Allergan, Genentech, Janssen, Regeneron, Regenix, Second Sight (consulting, grant); Pan Optica (consulting, grant, equity). Suber S. Huang: American Academy of Ophthalmology (consultant/advisor; Chair, AAO Research, Regulatory, Scientific Affairs committee during study); Asia Pacific Association of Ophthalmology, Santen, Spark Therapeutics, Volk (consultant/advisor); Diopsys (consultant/advisor, grant support, lecture fees); i2i Innovative Ideas, Inc (consultant/advisor, equity owner); Lumoptik (consultant, equity owner); NEHEP/NEI/NIH (consultant/advisor; Chair, National Eye Health Education Program); Regenerative Patch Technologies, RegenXBio (consultant/advisor; Chair, DMC); Second Sight (consultant/advisor; Independent Medical Safety Monitor). Mark S. Humayun: 1Co, Inc, oProbe, Reflow, Regenerative Patch Technologies, Replenish, Second Sight Medical Products, Inc (consultant/advisor, equity owner, patents/royalties); Alcon Laboratories Inc (consultant/advisor, lecture fees); Clearside, Allergan (consultant/advisor); Eyemedix (consultant/advisor, equity owner, patent/royalty, grant support); IRIDEX, Duke Eye Center, Johns Hopkins University (patents/royalties); Santen, Inc (consultant/advisor, speaker, honorarium); University of Southern California (employee, patents/royalty); Acucela (consultant/advisor, lecture fees). K. Thiran Jayasundera: NIH funding (K23 EY026985-01); Second Sight Medical Products, Inc, Editas Medicine (consultant). Gregg T. Kokame: Genentech (research support, consultant), Regeneron (research support, consultant, speaker); Bausch and Lomb, Second Sight, Bayer (consultant, speaker); Zeiss, Santen, Allergan, Ophthotech (consultant). Byron L. Lam: AGTC, Astellas, National Eye Institute, NightstaRx, Quark, Sanofi, Second Sight Medical Products, Inc (grant support); Shire (consultant/advisor, grant support); Ionis, Spark (consultant). Jennifer I. Lim: Alcon, Genentech, pSivida, Opthea, Quark, Kodiak, Santen, Pfizer/Hospira, Regeneron, Lumenis, Alexion, AbbVie, Alimera (consultant); Allergan, Janssen, Ohr, Second Sight, Regeneron, Genentech, Clearside (grants for UIC clinical trials); JAMA Ophthalmology Editorial Board, Vindico, CRC Press (honoraria). Naresh Mandava: Shape-tech LLC, Shape Ophthalmics LLC, 2C Tech corporation (founder, equity); Aurea Medical, LLC (founder, consultant, equity); ONL Therapeutics (consultant, equity). Sandra R. Montezuma: Second Sight Medical Products, Inc (consultant); Spark Therapeutics (advisory board). Lisa Olmos de Koo: Alcon Surgical R&D, ScienceBased Health (Scientific Advisory Board Member). Lejla Vajzovic: Novartis, Second Sight Medical Products, Inc, Roche (research grant); Regeneron, Janssen (consultant); Dutch Ophthalmic Research Center (honoraria, consultant). Peter Wiedemann: Bayer, Regeneron, Thrombogenics, Novartis, Allergan (clinical study grants). James Weiland: Platinum Group Coatings, LLC (ownership, consultant); Second Sight Medical Products, Inc (research collaboration). Jiong Yan: funding for MacTel study (NHOR, MacTel phase 2 and 3) from the Lowy Medical Foundation. David N. Zacks: ONL Therapeutics (equity, consulting, royalties); Foundation Fighting Blindness (research grant). The following authors have no financial disclosures: Natalia F. Callaway, Catherine Hoepfner, and Raymond Iezzi Jr. All authors attest that they meet the current ICMJE criteria for authorship.

Other Acknowledgments: The authors thank Jessy D. Dorn, PhD, and Cesia Toledo from Second Sight Medical Products, Inc (Sylmar, California, USA), for providing access to the Post-Market Surveillance Study images and administrative assistance for the current study.

REFERENCES

1. da Cruz L, Dorn JD, Humayun MS, et al. Five-year safety and performance results from the Argus II Retinal Prosthesis System Clinical Trial. *Ophthalmology* 2016;123(10):2248–2254.
2. Santos A, Humayun MS, de Juan E Jr, et al. Preservation of the inner retina in retinitis pigmentosa. A morphometric analysis. *Arch Ophthalmol* 1997;115(4):511–515.
3. Huang Q, Chowdhury V, Coroneo MT. Evaluation of patient suitability for a retinal prosthesis using structural and functional tests of inner retinal integrity. *J Neural Eng* 2009;6(3):035010.
4. Ahuja AK, Yeoh J, Dorn JD, et al. Factors affecting perceptual threshold in Argus II retinal prosthesis subjects. *Transl Vis Sci Technol* 2013;2(4):1–15.
5. da Cruz L, Coley BF, Dorn J, et al. The Argus II epiretinal prosthesis system allows letter and word reading and long-term function in patients with profound vision loss. *Br J Ophthalmol* 2013;97(5):632–636.
6. Duncan JL, Richards TP, Arditi A, et al. Improvements in vision-related quality of life in blind patients implanted with the Argus II Epiretinal Prosthesis. *Clin Exp Optom* 2017;100(2):144–150.
7. Gregori NZ, Davis JL, Rizzo S. Bimanual technique for retinal tacking of epiretinal prosthesis. *Retina* 2016;36(1):199–202.

8. Delyfer MN, Gaucher D, Govare M, et al. Adapted surgical procedure for Argus II retinal implantation: feasibility, safety, efficiency, and postoperative anatomic findings. *Ophthalmol Retina* 2017;1–12.
9. Seider MI, Hahn P. Argus II retinal prosthesis malrotation and repositioning with intraoperative optical coherence tomography in a posterior staphyloma. *Clin Ophthalmol* 2015; 9:2213–2216.
10. de Balthasar C, Patel S, Roy A, et al. Factors affecting perceptual thresholds in epiretinal prostheses. *Invest Ophthalmol Vis Sci* 2008;49(6):2303–2314.
11. Parmeggiani F, De Nadai K, Piovan A, Binotto A, Zamengo S, Chizzolini M. Optical coherence tomography imaging in the management of the Argus II retinal prosthesis system. *Eur J Ophthalmol* 2017;27(1):e16–e21.
12. Rachitskaya AV, Yuan A, Marino MJ, Reese J, Ehlers JP. Intraoperative OCT imaging of the Argus II Retinal Prosthesis System. *Ophthalmic Surg Lasers Imaging Retina* 2016; 47(11):999–1003.
13. Schatz A, Arango-Gonzalez B, Fischer D, et al. Transcorneal electrical stimulation shows neuroprotective effects in retinas of light-exposed rats. *Invest Ophthalmol Vis Sci* 2012;53(9): 5552–5561.
14. Morimoto T, Miyoshi T, Matsuda S, Tano Y, Fujikado T, Fukuda Y. Transcorneal electrical stimulation rescues axotomized retinal ganglion cells by activating endogenous retinal IGF-1 system. *Invest Ophthalmol Vis Sci* 2005;46(6): 2147–2155.
15. Chow AY, Chow VY, Packo KH, Pollack JS, Peyman GA, Schuchard R. The artificial silicon retina microchip for the treatment of vision loss from retinitis pigmentosa. *Arch Ophthalmol* 2004;122(4):460–469.
16. Willmann G, Schaferhoff K, Fischer MD, et al. Gene expression profiling of the retina after transcorneal electrical stimulation in wild-type Brown Norway rats. *Invest Ophthalmol Vis Sci* 2011;52(10):7529–7537.
17. Pardue MT, Phillips MJ, Yin H, et al. Possible sources of neuroprotection following subretinal silicon chip implantation in RCS rats. *J Neural Eng* 2005;2(1):S39–S47.
18. Goldberg JL, Espinosa JS, Xu Y, Davidson N, Kovacs GT, Barres BA. Retinal ganglion cells do not extend axons by default: promotion by neurotrophic signaling and electrical activity. *Neuron* 2002;33(5):689–702.
19. Gonzalez-Calle A, Weiland JD. Evaluation of effects of electrical stimulation in the retina with optical coherence tomography. *Conf Proc IEEE Eng Med Biol Soc* 2016;2016: 6182–6185.
20. Rodriguez M, Gregori NZ, Roisman L, Lam BL, Rosenfeld PJ. Swept-source OCT imaging of the Argus II Epiretinal Prosthesis. *Ophthalmol Retina* 2018;2(4):380–382.